

## YbH<sup>+</sup> formation in a ytterbium ion trap

Thai M. Hoang,<sup>1</sup> Yuan-Yu Jau,<sup>1</sup> Richard Overstreet,<sup>2</sup> and Peter D. D. Schwindt<sup>1</sup>

<sup>1</sup>*Sandia National Laboratories, Albuquerque, NM 87123, USA*

<sup>2</sup>*Microchip, Inc., Beverly, MA 01915, USA*

(Dated: July 2, 2019)

The trapped <sup>171</sup>Yb<sup>+</sup> ion is a promising candidate for portable atomic clock applications. However, with buffer-gas cooled ytterbium ions, the ions can become trapped in a low-lying <sup>2</sup>F<sub>7/2</sub>-state or form YbH<sup>+</sup> molecules. These dark states reduce the fluorescence signal from the ions and can degrade the clock stability. In this work, we study the dynamics of the populations of the <sup>2</sup>F<sub>7/2</sub>-state and YbH<sup>+</sup> molecules under different operating conditions of our <sup>171</sup>Yb<sup>+</sup> ion system. Our study indicates that <sup>2</sup>F<sub>7/2</sub>-state ions can form YbH<sup>+</sup> molecules through interactions with hydrogen gas. As observed previously, dissociation of YbH<sup>+</sup> is observed at wavelengths around 369 nm. We also demonstrate YbH<sup>+</sup> dissociation using 405-nm light. Moreover, we show the population in the dark states can be limited by using a single repump laser at 935 nm. Our study provides new insights into the molecular formation of a trapped ion system.

### INTRODUCTION

The past two decades have witnessed significant efforts in miniaturizing atomic clocks. There are several approaches to miniaturize an atomic clock such as laser cooled atoms [1–3], vapor-cell atomic clocks [4–7], and trapped ion clocks [8]. We focus on developing a highly miniaturized microwave atomic clock which is operated using the 12.6 GHz hyperfine ground state transition of trapped <sup>171</sup>Yb<sup>+</sup> ions [9–11]. Previous studies have shown that <sup>171</sup>Yb<sup>+</sup> ions can be trapped in the <sup>2</sup>F<sub>7/2</sub> state [12–20] and form a YbH<sup>+</sup> molecules [21, 22]. As a result, the <sup>171</sup>Yb<sup>+</sup> signal can be reduced and the clock stability is degraded. Understanding the <sup>2</sup>F<sub>7/2</sub>-state trapping and the YbH<sup>+</sup> molecular formation is one of the keys to the compact <sup>171</sup>Yb<sup>+</sup> atomic clock. Because of significant interest in the ytterbium ion, <sup>2</sup>F<sub>7/2</sub>-state trapping has been more broadly studied. In this paper, we investigate the YbH<sup>+</sup> formation of trapped ions.

Previous studies have suggested that YbH<sup>+</sup> molecular ions can be formed from the <sup>2</sup>F<sub>7/2</sub>-state or <sup>2</sup>D<sub>3/2</sub>-state ions through an interaction with hydrogen gas [21, 22]. Since it is difficult to completely remove hydrogen from a vacuum system, the YbH<sup>+</sup> formation can be problematic in a passively pumped vacuum package [9–11, 20]. We investigate the YbH<sup>+</sup> formation mechanism under different optical excitation conditions in such a passively pumped package. To optically excite the ions, 369-nm, 405-nm, 760-nm, and 935-nm lasers are used, and microwave radiation drives transitions within the <sup>2</sup>S<sub>1/2</sub> ground state. Primarily, we investigate the YbH<sup>+</sup> dynamics when both the optical and microwave radiation are applied continuously, and we compare our data to a rate equation model to understand the populations of the various states. We also perform a limited study of the populations when the lasers and microwave radiation are sequentially pulsed, and the rate equation is modified to account for only long-time-scale population dynamics. While our results do not

rule out formation of YbH<sup>+</sup> molecules from the <sup>2</sup>D<sub>3/2</sub>-state, our results suggest that YbH<sup>+</sup> are formed predominantly from <sup>2</sup>F<sub>7/2</sub>-state ions. Dissociation of YbH<sup>+</sup> has previously been observed at wavelengths of 369.48 nm, 369.44 nm, 369.20 nm, and 368.95 nm [14, 21, 22]. We demonstrate dissociation can also be achieved using 405-nm light from a free-running edge-emitting diode laser. Moreover, we illustrate that the 935-nm light can sufficiently prevent the molecular formation. Our study provides new insight into the molecular formation process and allows the determination of which lasers are necessary for the <sup>171</sup>Yb<sup>+</sup> atomic clock operation.

### EXPERIMENTAL SYSTEM

The experiments are carried out in a 3-cm<sup>3</sup> vacuum package developed and constructed by the Jet Propulsion Laboratory (Figure 1b). The vacuum package is permanently sealed with a copper pinch-off and passively pumped with a nonevaporable getter. The <sup>171</sup>Yb<sup>+</sup> ions are trapped in a linear quadrupole RF Paul trap which has 240 V<sub>rms</sub> applied between adjacent trap rods at 3.35 MHz, and the four trap rods are held at a -20V potential difference relative the grounded end cap electrodes of the trap. The vacuum package details are described in Refs. [9–11]. The vacuum package is filled with 4 × 10<sup>-6</sup> Torr of neon (as read from an ion gauge without a gas correction factor applied), which provides buffer gas cooling of the ions. Microwave radiation is applied to the ions by coupling the microwave power into the package through the trap rods. The 935-nm laser (~ 0.5 mW) is used to clear the low-lying <sup>2</sup>D<sub>3/2</sub> state, and the 760-nm laser (~ 0.5 mW) is used to clear the <sup>2</sup>F<sub>7/2</sub> state. The 369-nm laser is used for state detection and optical pumping. A 250-mm focal lens is used to focus these laser beams at the ion cloud. Fluorescence of trapped ions at 369-nm is collected using a photomultiplier tube. The Yb<sup>+</sup> ion signal is detected using the 369-nm fluorescence.

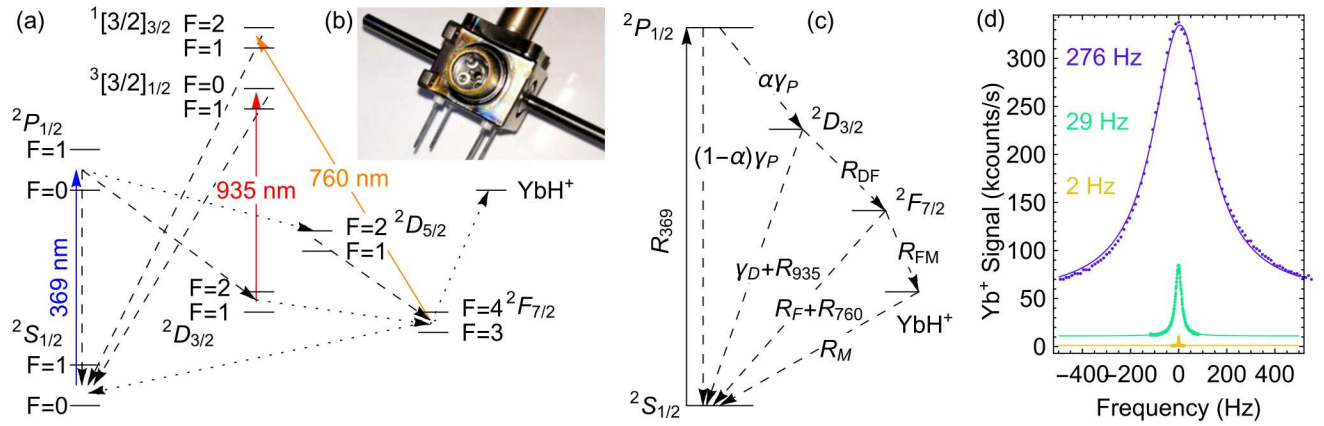


FIG. 1. (a) Simplified energy level diagram of the  $^{171}\text{Yb}^+$  ion. The solid arrows show the laser transitions. The dashed arrows show the spontaneous decays. The dotted arrows show collisional decays. (b) Photograph of the  $3\text{ cm}^3$  vacuum package. (c) A simplified rate equation diagram illustrates the levels and the transitions used in the rate equation model. (d) Microwave linewidth measurements. The data (circle markers) are fitted to the Lorentzian function (solid line). The numbers indicate the full width at half maximum of the fits. Each measurement is represented by a different color.

## THEORETICAL MODEL

To understand the  $\text{YbH}^+$  formation, we first consider the transitions between different energy levels of a  $^{171}\text{Yb}^+$  ion under optical excitation (Figure 1a). Without the hyperfine structure, the energy diagram can be simplified as shown in Figure 1c. Assuming that  $\text{YbH}^+$  molecular ions are formed from  $F$ -state ions, the rate equations can be written as,

$$\begin{aligned}
 \dot{n}_S &= -R_{369}n_S + (1 - \alpha)\gamma_P n_P + (\gamma_D + R_{935})n_D \\
 &\quad + (R_F + R_{760})n_F + R_M n_M \\
 \dot{n}_P &= -\gamma_P n_P + R_{369}n_S \\
 \dot{n}_D &= -(\gamma_D + R_{935} + R_{DF})n_D + \alpha\gamma_P n_P \\
 \dot{n}_F &= -(R_F + R_{760})n_F + R_{DF}n_D - R_{FM}n_F \\
 \dot{n}_M &= R_{FM}n_F - R_M n_M.
 \end{aligned} \tag{1}$$

Here  $n_S, n_P, n_D, n_F,$  and  $n_M$  are the relative population of the  $S_{1/2}, P_{1/2}, D_{3/2}, F_{7/2},$  and  $\text{YbH}^+$  states. The branching ratio of the  $P$ -state to the  $D$ -state,  $\alpha$ , is  $\sim 0.005$  [20]. The spontaneous decay of the  $P$ -state and  $D$ -state are  $\gamma_P$  ( $\sim 10^8\text{ s}^{-1}$ ) and  $\gamma_D$  ( $\sim 20\text{ s}^{-1}$ ), respectively.  $R_{369}$  is the effective pumping rate of the 369-nm laser and the microwave radiation combined. The optical pumping rate of the 760-nm and 935-nm lasers is  $R_{760}$  ( $\sim 10^{-1}\text{ s}^{-1}$ ) and  $R_{935}$  ( $\sim 10^3\text{ s}^{-1}$ ), respectively. The rates from the  $D \rightarrow F, F \rightarrow \text{YbH}^+, F \rightarrow S,$  and  $\text{YbH}^+ \rightarrow S$  states are  $R_{DF}, R_{FM}, R_F,$  and  $R_M$ , respectively.

For much of this study the clock was operated in a “continuous mode,” where the 12.6 GHz microwave radiation and the resonant 369-nm light continuously illuminate the ions. The full width at half maximum (FWHM) of the clock resonance is determined by optical and mi-

crowave power broadening,

$$FWHM = \frac{1}{\pi} \sqrt{\frac{\beta}{2} \Omega^2 + \left(\frac{\Gamma_{369}}{2}\right)^2} \tag{2}$$

where  $\Omega$  is the microwave Rabi frequency,  $\Gamma_{369}$  is the pumping rate of the 369-nm laser from the  $|^2S_{1/2}, F=1\rangle$  state to either hyperfine level of the  $|^2P_{1/2}\rangle$  state, and  $\beta$  is the average number of photons scattered before optical pumping to the  $|^2S_{1/2}, F=0, m_F=0\rangle$  state. For the  $|^2S_{1/2}, F=1\rangle$  to  $|^2P_{1/2}, F=1\rangle$  (1-to-1 transition),  $\beta=3$ , while for the  $|^2S_{1/2}, F=1\rangle$  to  $|^2P_{1/2}, F=0\rangle$  transition (1-to-0 transition)  $\beta=300$  to 500, depending on the ion temperature. In the photon shot-noise limit, the signal-to-noise ratio at a given FWHM is optimized when  $\Gamma_{369} = \pi FWHM$  and  $\Omega = \sqrt{3/(2\beta)}\pi FWHM$ , and in the experiment we set the 369-nm laser and microwave power to these levels, which gives  $R_{369} = \frac{3}{8}\pi FWHM$ . The time to optically pump the ions from the upper clock state to the lower state is  $\beta/(\pi FWHM)$ . Thus, the 1-to-1 transition can be used to interrogate the clock transition much faster than the 1-to-0 transition in a continuous mode. However, in the continuous mode many fewer photons are scattered per microwave photon absorbed compared to a “pulsed mode” of operation, where the microwave radiation and the 369-nm laser light are sequentially applied. In this paper, the 1-to-1 transition and the 1-to-0 transition are used in the continuous mode and the pulsed mode, respectively. A more thorough discussion of the pulsed and continuous mode is found in Ref. [23]. To determine value of  $R_{369}$ , we measure the microwave linewidth for a given 369-nm power used in the experiment. In the paper, we operate with  $R_{369} = \frac{1}{3}\pi FWHM$ . A sample of the microwave linewidths from 2 Hz up to 276 Hz is shown in Figure 1d. The 369-nm power increases from a few nW to hundreds nW as the microwave linewidth is increased from a few Hz to a few hundred Hz.

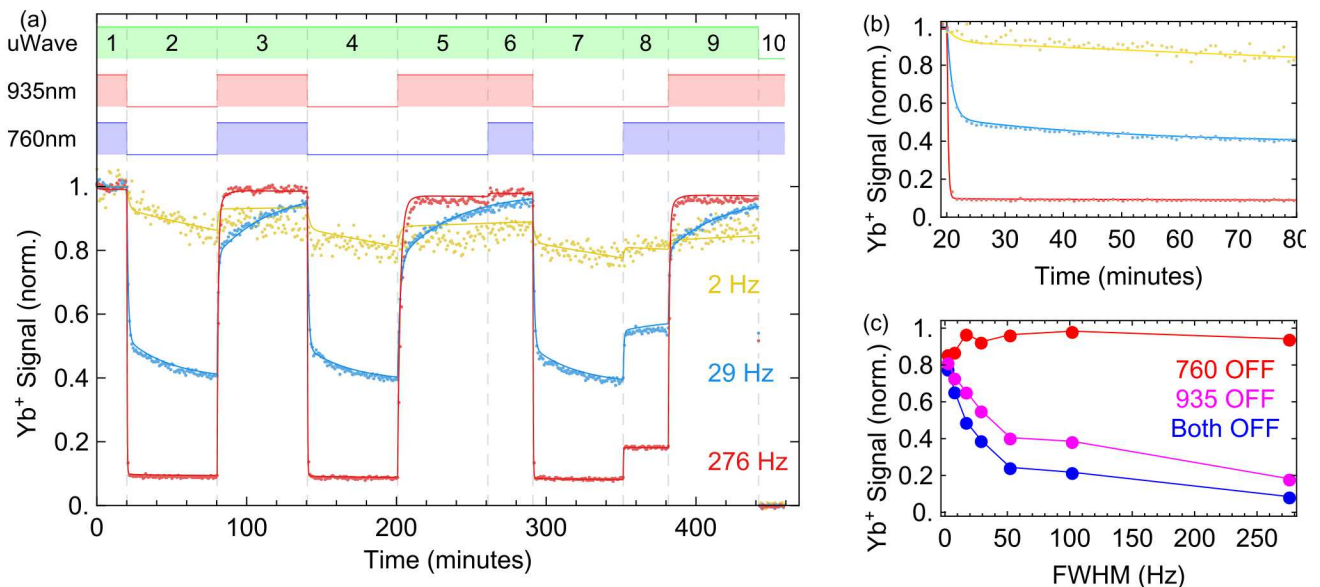


FIG. 2. (a) Normalized Yb fluorescence signal for different microwave linewidths. The data (circular markers) are compared to the the simulations (solid lines) to obtain the best free parameters. The state (on/off) of the microwave radiation, the 935-nm laser, and the 760-nm laser are represented by the respective green, red, and blue shaded regions at the top of the plot. The dashed lines divide the experiment into small segments labeled by numbers from 1 to 10. The background level is determined by turning off the microwave radiation. (b) The Yb signal of segment 2 in plot (a). (c) Comparing the fractional Yb signals at varying linewidths of the microwave transition. Data show the fractional signals without the 760-nm laser at the end of the segment 5 (red markers), without the 935-nm laser at the end of segment 8 (magenta markers), and without both of the lasers at the end of segment 7 (blue markers).

## POPULATION DYNAMICS AND THE MOLECULAR ION FORMATION

### Population dynamics

To understand the molecular formation mechanism, we optically excite  $^{171}\text{Yb}^+$  ions and observe the  $\text{Yb}^+$  ion signal under different excitation scenarios (Figure 2a). We perform experiments for different microwave linewidths (2 Hz, 29 Hz, and 276 Hz) using the 1-to-1 transition. To monitor the ion signal, the  $^{171}\text{Yb}^+$  ions are continuously pumped from the  $S$ -state to the  $P$ -state by the 369-nm laser. The  $\text{Yb}^+$  ion signal is detected by collecting the 369-nm photons spontaneously emitted from the  $P$ -state to  $S$ -state. Here, the background level is determined by turning off the microwave radiation. The microwave-off signal yields a similar photon count as detuning the 369-nm laser away from the 1-to-1 transition. Since the spontaneous emission occurs extremely fast ( $\sim 10^8 \text{ s}^{-1}$ ) compared to the optical pumping rate ( $10^2 \text{ s}^{-1}$  or less), the steady-state fractional population of the  $P$ -state is nearly zero. The  $\text{Yb}^+$  ion signal normalized to unity reflects the fraction of the population in the  $S$ -state.

To validate that molecular ions are formed from the  $F$ -state ions, we compare data to the numerical simulation of Equation 1. Here  $R_{DF}$ ,  $R_F$ ,  $R_{FM}$ ,  $R_M$ , and  $R_{760}$  are free parameters of the rate equation. We first focus on

the segment 2 of Figure 2a which is enlarged in Figure 2b. As the 760-nm and 935-nm lasers are turned off, the Yb fluorescence signal will decay. To roughly estimate the free parameters, we use the 29 Hz linewidth data since this data set has an obvious double decay feature. The fast decay occurring within the first few minutes is due the  $F$ -state trapping [18–20]. The ratio of  $R_F$  and  $R_{DF}$  determines the normalized ion signal after the fast decay. The sum  $R_F + R_{DF}$  determines the ion signal decay rate. We attribute the slow decay on an hour timescale to the  $\text{YbH}^+$  formation. The ratio of  $R_M$  and  $R_{FM}$  determines the ion signal steady-state value, and the sum  $R_M + R_{FM}$  determines the ion signal decay rate. Starting from this initial estimation, we perform the simulations iteratively to determine the free parameters. The free parameters are determined by minimizing the root-mean-square error (RMSE) between the data and the simulation. We estimate that  $R_{DF} \approx 1.25 \text{ s}^{-1}$ ,  $R_F \approx 9.6 \times 10^{-3} \text{ s}^{-1}$ ,  $R_{760} \approx 13 \times 10^{-3} \text{ s}^{-1}$ ,  $R_{FM} \approx 0.28 \times 10^{-3} \text{ s}^{-1}$ , and  $R_M \approx 0.45 \times 10^{-3} \text{ s}^{-1}$ .  $R_{760}$  is determined using the segment 8 in the Figure 2a. Once the free parameters are determined for the 29 Hz linewidth data, we use the same free parameters  $R_{DF}$ ,  $R_F$ ,  $R_{760}$  and  $R_{FM}$  for the 2 Hz and 276 Hz simulations. Since the molecular ions can be disassociated by the 369 nm light, we assume that an effective disassociation rate  $R_M$  is proportional to  $R_{369}$ , which is proportional to the 369-nm optical power. Over-

all, the data agree well with the numerical simulation. This result suggests that the  $^{171}\text{Yb}^+$  molecular ions are formed largely from the  $F$ -state ions since molecular formation from the  $D$ -state is not included in the numerical model. Previous work has suggested that the molecular ions can be formed from the  $D$ - or  $F$ -states through an interaction with hydrogen gas [22]. This is discussed in more detail below.

Moreover, the data indicate that the 760-nm has little effect on the 369-nm fluorescence signal (Figure 2c). The Yb signal does not show a significant reduction under the absence of the 760-nm laser. This indicates that the  $^{171}\text{Yb}^+$  ion clock may be operated in a continuous mode without the 760-nm laser. The 935-nm laser alone can maintain the Yb signal at a sufficient level. When the microwave linewidth is less than a few Hz, the 369-nm fluorescence signal does not reduce much as we turn off both the 935-nm and 760-nm lasers. The 369-nm fluorescence signal only reduces by 20%. However, it is important to note that these behaviors depend the exact composition of the gases within the vacuum package. If the decay rate out of the  $F$ -state back to the  $S$ -state  $R_F$  is too slow, an  $F$ -state clearing laser may be required, and  $R_F$  depends on the background gas composition. Since our vacuum package is permanently sealed, the exact composition in this package is not known.

### Comparing $D \rightarrow \text{YbH}^+$ and $F \rightarrow \text{YbH}^+$ simulations

To further verify that the molecular ions are formed primarily from the  $F$ -state ions, we perform a  $D \rightarrow \text{YbH}^+$  simulation where  $\text{YbH}^+$  ions are formed only from ions in the  $D$ -state. Comparing the  $D \rightarrow \text{YbH}^+$  simulation to the  $F \rightarrow \text{YbH}^+$  simulation, they both agree well to the 29 Hz linewidth data through segment 7 in Figure 3. However, the  $D \rightarrow \text{YbH}^+$  simulation does not agree to the data at the segment 8 and 9 (Figure 3b). In the segment 8, the 760-nm laser is turned on after blocking both the 760-nm and 935-nm lasers for a long period. The  $D \rightarrow \text{YbH}^+$  model predicts that the 369-nm fluorescence signal will increase rapidly right after the 760-nm is turned when ions are cleared out of the  $F$ -state. The ions then will be transferred quickly into the  $D$ -state (Figure 1c). From the  $D$ -state, the ions would form the  $\text{YbH}^+$  molecular ions. As a result, the  $\text{Yb}^+$  signal should slowly decrease after an initial jump. However, the  $\text{Yb}^+$  signal does not decrease like the  $D \rightarrow \text{YbH}^+$  model predicts. The  $\text{Yb}^+$  signal instead slightly increases, which is more consistent with the  $F \rightarrow \text{YbH}^+$  simulation. Since the 760-nm laser clears  $F$ -state ions, the molecular formation from  $F$ -state ions will be reduced. As the result, the ion signal increases when  $\text{YbH}^+$  molecules are disassociated back to  $\text{Yb}^+$  ions. Note that our experiment does not rule out the possibility of  $\text{YbH}^+$  formation from  $D$ -state ions but shows that  $F \rightarrow \text{YbH}^+$  is the dominant

process.

### Disassociating $\text{YbH}^+$ molecules

Previous studies have shown that the  $\text{YbH}^+$  molecular ions can be disassociated using 369 nm light tuned to particular resonant wavelengths [14, 21, 22]. The disassociation wavelengths occur at 369.48 nm, 369.44 nm, 369.20 nm, and 368.95 nm. We perform dissociation spectroscopy to detect  $\text{YbH}^+$  molecules using a laser tuned to the 369.48-nm wavelength. For this experiment two 369-nm lasers are used. First, the ions are exposed to 50–76  $\mu\text{W}$  of light to dissociate the molecules. Then, the second laser is applied on resonance with the 1-to-1 transition (at 369.5251 nm) to monitor the ion signal after the disassociation period. The 760-nm laser is on while the 935-nm laser is blocked. If the molecular disassociation occurs, the number of  $\text{Yb}^+$  ions will increase. As a result, the ion signal will increase.

As we scan the 369-nm laser across the 369.48 nm disassociation wavelength, the ion signal shows a resonance peak at 369.482 nm (Figure 4a). This is an indication of the  $\text{YbH}^+$  disassociation. This observation is consistent with the earlier studies [14, 21, 22]. When the disassociation time is prolonged to 6 seconds, the disassociation linewidth is broadened. With a 0.5 second of disassociation time, the resonance peak has a FWHM of about 15 pm (33 GHz). The FWHM is broadened to about 100 pm for a 6 second disassociation. This indicates that the molecular ions can be disassociated using off-resonant light.

Since the  $\text{Yb}^+$  signal is collected using the 369-nm photons emitted from trapped ions, using 369-nm light for the molecular disassociation will increase background noise. For a  $\text{Yb}^+$  ion clock, a high background level will degrade the clock stability. For this reason, we demonstrate that 405-nm light can disassociate  $\text{YbH}^+$ . Using a free-running edge-emitting diode laser, we apply 405-nm light to the trapped ions for 10 second with varying power. The ion signal increases to a steady level after the 405-nm laser power reaches above a 1 mW level (Figure 4b). We also compare the disassociation process with and without the 760-nm laser. If the 405-nm light could clear the  $F$ -state, the  $\text{Yb}^+$  signal with the 760-nm laser should be higher than that without the 760-nm laser. Since the results with and without the 760-nm are comparable, the  $\text{Yb}^+$  signal increases mainly due to the  $\text{YbH}^+$  disassociation.

We also compare the  $\text{Yb}^+$  signal with and without the 405-nm laser using the same procedure in Figure 2. We will first focus on segment 2 of Figure 4c, where both the 760-nm and 935-nm lasers are blocked, to illustrate the effect of the 405-nm laser. When the 405-nm laser is absent, the trapped ions will quickly fall into the  $F$ -state [18–20] and then slowly form  $\text{YbH}^+$  as discussed in the

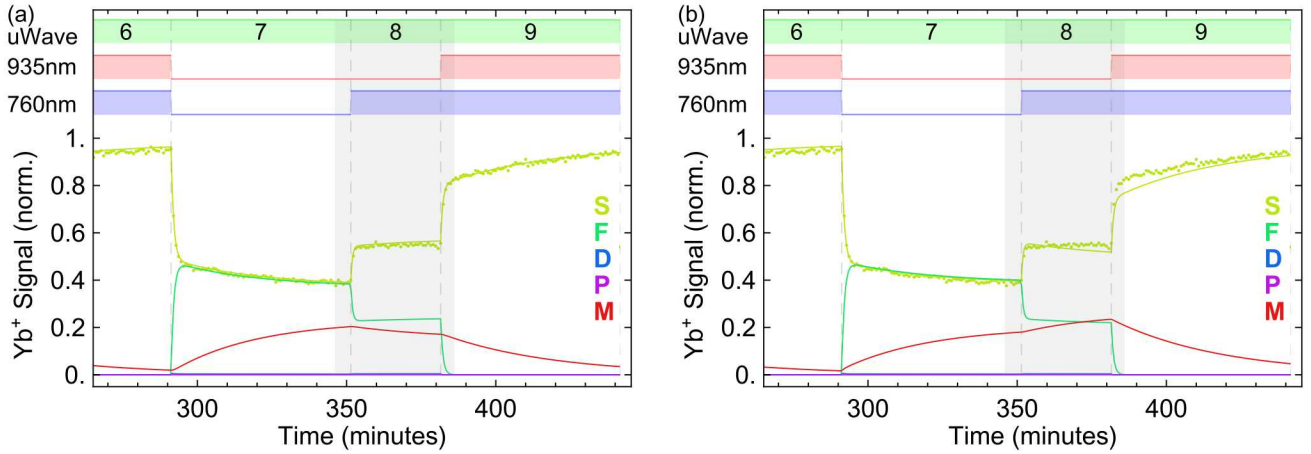


FIG. 3. Comparing the  $F \rightarrow \text{YbH}^+$  simulation model (a) and the  $D \rightarrow \text{YbH}^+$  simulation model (b). The data (circular markers) are compared to the the simulations (solid lines) to obtain the best free parameters. The microwave, the 935-nm laser, and the 760-nm laser states are represented by green, red, and blue bars respectively. The dashed lines divide the experiment into small segments labeled by numbers from 6 to 9. The simulated populations of the different energy states are represented by different colors. The colored letters represent the corresponding  $\text{YbH}^+$ ,  $P$ ,  $D$ ,  $F$ , and  $S$  states. The Yb signal (norm.) is normalized to unity.

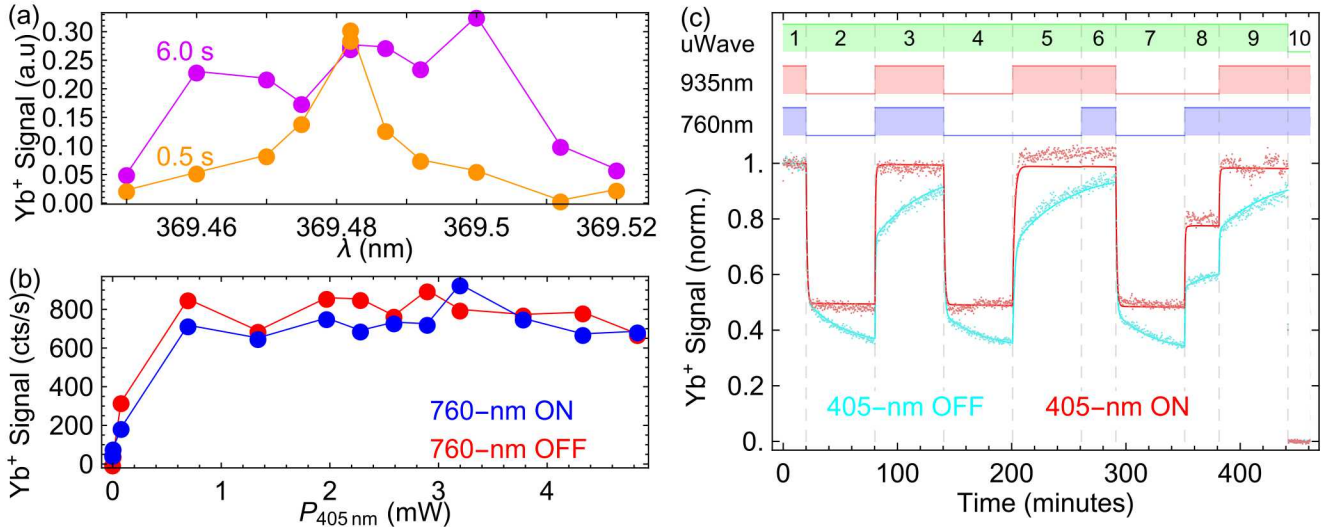


FIG. 4. (a) Plot of molecular dissociation using the 369-nm light. The colored numbers indicate the total time that the ions are exposed to the 369-nm light. For a 0.5 second disassociation, the Yb signal peaks at 369.482 nm. The molecular ions can be disassociated even with off-resonant light if the molecular ions are exposed to the 369-nm light longer. Here the power of the disassociation laser is about 50–76  $\mu\text{W}$ . (b) The molecular ion dissociation with 405 nm. The molecular ions are exposed to the 405-nm light for 10 seconds. The beam waist diameter is about 1.4 mm. The red (blue) points are when the 760-nm laser is off (on) (c) Fractional Yb signal at a 30 Hz linewidth with and without the 405-nm disassociation laser. The 405-nm laser power is 2.7 mW. The data (circle markers) are compared to the the simulations (solid lines) to obtain the best free parameters that minimize the error variance of the simulation and the data. When the 405 nm light is on, the rate of forming  $\text{YbH}^+$  is assumed to be zero. The microwave, the 935-nm laser, and the 760-nm laser are represented by green, red, and blue pulses respectively. The dashed lines divide the experiment into small segments labeled by numbers from 1 to 10.

previous section. The  $\text{Yb}^+$  signal without the 405-nm laser shows the double decay time constants as expected. On the other hand, the 405-nm laser will significantly increase the  $\text{YbH}^+$  dissociation rate. When the  $\text{YbH}^+$  disassociation rate is much faster than the  $\text{YbH}^+$  formation rate, the  $\text{YbH}^+$  population is negligible. Under the

presence of high 405-nm laser power, the trapped ions will quickly fall into the  $F$ -state with a negligible  $\text{YbH}^+$  population. The data show that the  $\text{Yb}^+$  signal quickly decays to a steady state due to the  $F$ -state trapping. Overall, the data show a good agreement with the numerical simulation of Equation [1](#). Here we fit the without

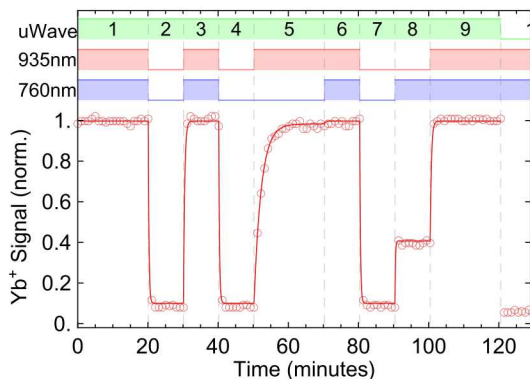


FIG. 5. a, Normalized Yb fluorescence signal in the pulse mode operation (1.45 second of microwave and 0.25 second of 369-nm light). The fluorescence signal is collected in the first 10 ms after the light is turned on. The 369-nm power is  $\sim 10 \mu W$ , which yields an optical pumping time of 23 ms. The microwave power, the 935-nm laser, and the 760-nm laser are represented by green, red, and blue bars respectively. The dashed lines divide the experiment into small segments labeled by numbers from 1 to 10. The data (circle markers) are compared to the numerical simulation (solid line). The background level is determined by detuning the 369-nm laser away from the 1-to-0 transition.

405-nm laser data to the theoretical model to obtain the free parameters. We use the same parameters to simulate the population dynamics under the presence of the 405-nm laser. To include the molecular dissociation effect of the 405-nm laser, we simply change the molecular dissociation rate  $R_M$ . The data with 405-nm laser agrees well to the numerical simulation when the  $R_M$  rate is about 20 times larger than the molecular formation rate  $R_{FM}$ .

### Pulsed mode operation

Since a ytterbium ion clock is often operated in the pulsed mode, we will briefly discuss the population dynamics under the pulsed mode operation. In the pulsed mode operation, either a single Rabi to two Ramsey microwave pulses are applied to the ions followed by a 369-nm light pulse. We typically apply a single pulse, which transfers ions from the  $|^2S_{1/2}, F=0\rangle$  state to the  $|^2S_{1/2}, F=1\rangle$  state, and fluorescence collected during the 369-nm light pulse determines the relative populations of the two states. Since the 369-nm light is off during the microwave interrogation, the pulsed mode does not suffer the light shift problem as in the continuous mode operation. In the pulsed mode operation, we apply  $10 \mu W$  of 369-nm power which optically pumps the ions back to the  $|^2S_{1/2}, F=0\rangle$  with a time constant of  $\sim 23$  ms. Figure 5 shows the  $Yb^+$  signal in the pulsed mode operation (1.45 s of microwave and 0.25 s of 369-nm light).

Rather than a full multi-state model, we implement a simplified two level model that includes only the  $S$ -state and the  $F$ -state as described in Ref. [20]. Since the  $10 \mu W$  of 369-nm light can disassociate  $YbH^+$  quickly, the  $YbH^+$  population is not considered. With the rapid spontaneous decay of the  $P$ -state, the population of the  $P$ -state is nearly zero. Also, the decay rate of the  $D$ -state is much faster than those rates associated with going into and out of the  $F$ -state, so the short time-scale dynamics of the  $D$ -state is neglected and the  $D$ -state population is given as a fraction  $\alpha_D$  of the  $S$ -state. In this way, we only consider the steady-state populations after each pulse, and the long-time-scale pulsed mode dynamics is given by modifying Equation 1 as,

$$\begin{aligned} \dot{n}_S &= -\alpha_D r_{DF} n_S + (r_F + r_{760} + r_{FM}) n_F \\ \dot{n}_F &= -(r_F + r_{760} + r_{FM}) n_F + \alpha_D r_{DF} n_S. \end{aligned} \quad (3)$$

Since  $\alpha_D$  is the fraction of the  $S$ -state population in the  $D$ -state, it will depend on the ratio of the microwave pulse length to the 369-nm laser pulse length, the 369-nm laser power, and the 935-nm laser power, which clears ions out of the  $D$ -state. Adding the parameter  $\alpha_D$  into Equation 3 is equivalent to adjusting the effective rate going from  $S$ -state to  $F$ -state due to the 2-level simplification. Moreover, ions in the  $D$ -state, the  $P$ -state, and the  $YbH^+$  form also decay into the  $S$ -state during the pulse mode operation. In general, the effective rates from  $F$ -state to  $S$ -state have to be adjusted to compensate for the ignored states in the 2-level model. Here  $r_{DF}$ ,  $r_F$ ,  $r_{FM}$ , and  $r_{760}$  are the effective rates from  $F$ -state to  $S$ -state, which corresponds to  $R_{DF}$ ,  $R_F$ ,  $R_{FM}$ , and  $R_{760}$  of the continuous mode, respectively. The data agrees well to the numerical simulation of Equation 3 when  $r_F = 7.7 \times 10^{-3} s^{-1}$ ,  $r_{760} = 41 \times 10^{-3} s^{-1}$ ,  $r_{FM} = 0.28 \times 10^{-3} s^{-1}$ ,  $r_{DF} = 1.25 s^{-1}$ , and

$$\alpha_D = \begin{cases} 113 \times 10^{-6}, & 935 - \text{nm ON}, \\ 60 \times 10^{-3}, & 935 - \text{nm OFF}. \end{cases}$$

Here these parameters are obtained by minimizing the RMSE between the data and the simulation. Overall, the parameters are similar with the those found for the continuous mode data. The effective pumping rate  $R_{760}$  of the pulse mode data is about 3 times higher than that of the continuous mode data. This difference is an effect of the 2-level simplification as we discussed above. We note that to obtain a more precise description of the pulse mode dynamics, a simulation including all energy levels should be used while observing the fluorescence decay for each pulse of the 369-nm laser. Since this type of simulation requires a small integration step ( $< 10^{-2} s$ ), it is not ideal to simulate a few hours of experimental data. Finally, while the vacuum package used in this work had little  $F$ -state trapping without the use of the 760-nm laser, other sealed vacuum packages required the 760-nm laser to avoid significant  $F$ -state populations. The

$F$ -state trapping we assume depends on the exact gas background in the package, which depends on the details of the preparation of the vacuum package and how long since it has been sealed.

## CONCLUSION

In conclusion, we have demonstrated that the formation of  $\text{YbH}^+$  molecular ions occurs when the ytterbium ions are primarily in the  $F$ -state. The experimental data show good agreement with the theoretical model that has no  $\text{YbH}^+$  formation out of the  $D$ -state. Our study indicates that the 760-nm has little effect on  $\text{Yb}^+$  ions when the 369-nm power is low. Since 935-nm light can clear ions out of the  $D$ -state, it can stop ions going into the  $F$ -state from the  $D$ -state. If the ions are not trapped in the  $F$ -state, they will not likely form  $\text{YbH}^+$  molecules. Therefore, it is possible to run a  $\text{Yb}^+$  atomic clock in a continuous mode using only a 369-nm and 935-nm laser. We also demonstrate that  $\text{YbH}^+$  molecules can be dissociated using an off-resonant 405-nm light. With the permanently sealed vacuum packages used in our work, the exact composition of the gas background can change from package to package giving different rates for  $R_F$ ,  $R_{DF}$ ,  $R_M$ , and  $R_{FM}$ . Once these rates are known, our model can determine how to minimize the number of molecular ions and  $\text{Yb}$  ions in the  $F$ -state. Our results provide new insights into the trapped  $\text{Yb}^+$  ion system which can be applied to improve the  $\text{Yb}^+$  atomic clock whether it is operating in the continuous mode or the pulsed mode. The molecular ion study can also be applied to other trapped ion systems.

## ACKNOWLEDGMENT

The authors would like to thank Jeff Hunker for assembling various parts of the apparatus. This research was developed with funding from the Defense Advanced Research Projects Agency (DARPA). The views, opinions and/or findings expressed are those of the authors and should not be interpreted as representing the official views or policies of the Department of Defense or the U.S. Government. Sandia National Laboratories is a multi-mission laboratory managed and operated by National Technology and Engineering Solutions of Sandia, LLC, a wholly owned subsidiary of Honeywell International, Inc., for the U.S. Department of Energy's National Nuclear Security Administration under contract DE-NA0003525.

*trol Symposium (IFCS), 2016 IEEE International*, 1–6 (IEEE, 2016).

- [2] Liu, X., Ivanov, E., Yudin, V. I., Kitching, J. & Donley, E. A. Low-drift coherent population trapping clock based on laser-cooled atoms and high-coherence excitation fields. *Phys. Rev. Appl.* **8**, 054001 (2017).
- [3] Scherer, D. R. *et al.* Progress on a miniature cold-atom frequency standard. *arXiv preprint arXiv:1411.5006* (2014).
- [4] Knappe, S. *et al.* A microfabricated atomic clock. *Appl. Phys. Lett.* **85**, 1460–1462 (2004).
- [5] Lutwak, R. *et al.* The miniature atomic clock-production results. In *Frequency Control Symposium, 2007 Joint with the 21st European Frequency and Time Forum. IEEE International*, 1327–1333 (IEEE, 2007).
- [6] Maleki, L. *et al.* All-optical integrated rubidium atomic clock. In *Frequency Control and the European Frequency and Time Forum (FCS), 2011 Joint Conference of the IEEE International*, 1–5 (IEEE, 2011).
- [7] Phelps, G., Lemke, N., Erickson, C., Burke, J. & Martin, K. Compact optical clock with  $5 \times 10^{-13}$  instability at 1 s. *Navigation: Journal of The Institute of Navigation* **65**, 49–54 (2018).
- [8] Prestage, J. D. & Weaver, G. L. Atomic clocks and oscillators for deep-space navigation and radio science. *Proceedings of the IEEE* **95**, 2235–2247 (2007).
- [9] Jau, Y.-Y. *et al.* Low-power, miniature  $^{171}\text{Yb}$  ion clock using an ultra-small vacuum package. *Appl. Phys. Lett.* **101**, 253518 (2012).
- [10] Schwindt, P. D. *et al.* A highly miniaturized vacuum package for a trapped ion atomic clock. *Rev. Sci. Instrum.* **87**, 053112 (2016).
- [11] Schwindt, P. D. *et al.* Miniature trapped-ion frequency standard with  $^{171}\text{Yb}^+$ . In *Frequency Control Symposium & the European Frequency and Time Forum (FCS), 2015 Joint Conference of the IEEE International*, 752–757 (IEEE, 2015).
- [12] Lehmitz, H., Hattendorf-Ledwoch, J., Blatt, R. & Harde, H. Population trapping in excited  $\text{yb}$  ions. *Phys. Rev. Lett.* **62**, 2108 (1989).
- [13] Klein, H., Bell, A., Barwood, G., Gill & P. Laser cooling of trapped  $\text{yb}^+$ . *Appl. Phys. B* **50**, 13–17 (1990).
- [14] Bauch, A., Schnier, D. & Tamm, C. Collisional population trapping and optical deexcitation of ytterbium ions in a radiofrequency trap. *J. Mod. Opt.* **39**, 389–401 (1992).
- [15] Tamm, C. A tunable light source in the 370 nm range based on an optically stabilized, frequency-doubled semiconductor laser. *Appl. Phys. B* **56**, 295–300 (1993).
- [16] Bell, A., Gill, P., Klein, H., Levick, A. & Rowley, W. Precision measurement of the  $^2f_{7/2} - ^2d_{5/2}$  2.43  $\mu\text{m}$  interval in trapped  $^{172}\text{Yb}^+$ . *J. Mod. Opt.* **39**, 381–387 (1992).
- [17] Seidel, D. & Maleki, L. Efficient quenching of population trapping in excited  $\text{Yb}^+$ . *Phys. Rev. A* **51**, R2699 (1995).
- [18] Yu, N. & Maleki, L. Lifetime measurements of the  $4f^{14}5d$  metastable states in single ytterbium ions. *Phys. Rev. A* **61**, 022507 (2000).
- [19] Schauer, M. M. *et al.* Collisional population transfer in trapped  $\text{Yb}^+$  ions. *Phys. Rev. A* **79**, 062705 (2009).
- [20] Jau, Y.-Y., Hunker, J. & Schwindt, P.  $F$ -state quenching with  $\text{ch}_4$  for buffer-gas cooled  $^{171}\text{Yb}^+$  frequency standard. *AIP Advances* **5**, 117209 (2015).

---

[1] Sebbly-Strabley, J. *et al.* Design innovations towards miniaturized gps-quality clocks. In *Frequency Con-*

- [21] Sugiyama, K. & Yoda, J. Disappearance of  $\text{Yb}^+$  in excited states from rf trap by background gases. *Jpn. J. Appl. Phys.* **34**, L584 (1995).
- [22] Sugiyama, K. & Yoda, J. Production of  $\text{YbH}^+$  by chemical reaction of  $\text{Yb}^+$  in excited states with  $\text{H}_2$  gas. *Phys. Rev. A* **55**, R10 (1997).
- [23] Schwindt, P. D., Hoang, T. M., Jau, Y.-Y. & Overstreet, R. Operating a  $^{171}\text{Yb}^+$  microwave ion clock in a continuous mode. In *2018 IEEE International Frequency Control Symposium (IFCS)*, 1–4 (IEEE, 2018).